

Non-linear analysis of steel-concrete composite frames via RPHM considering cracking and partial shear connection

Pedro H.A. Lima¹, Tawany A. Carvalho¹, Ígor J.M. Lemes¹, Rafael C. Barros², Ricardo A.M. Silveira²

¹Dept. of Engineering, Federal University of Lavras
Campus Universitário, Lavras, 37200-000, Minas Gerais, Brasil
peha.lima@gmail.com, tawanyacarvalho@gmail.com, igor.lemes@ufla.br

²Dept. of Civil Engineering, Federal University of Ouro Preto
Campus Morro do Cruzeiro, Ouro Preto, 35400-000, Minas Gerais, Brasil
rafael.barros@ufop.edu.br, ricardo@em.ufop.br

Abstract. The present work aims at the implementation and validation of a two-dimensional numerical formulation for the simulation of steel-concrete composite frames. Geometric and material nonlinearities are considered. A corotational approach is used to simulate second order effects. In the case of material nonlinearity, zero-length pseudo springs are used at the finite elements ends, where the gradual loss of flexural stiffness is determined by the combination of normal and flexural efforts (NM) at the nodal points, exclusively. The limits of the non-cracked, elastic and plastic regimes of the section are made in the NM interaction diagram. This diagram is obtained from the Strain Compatibility Method (SCM), where the non-linear analysis of the cross section is made. The cracking of the concrete is explicitly simulated with the effective moment of inertia proposed by NBR 6118 (2014). For steel-concrete composite beams, the possibility of longitudinal sliding between the concrete slab and the steel profile is considered, with the degradation of inertia being addressed as prescribed in NBR 8800 (2008). The results obtained are compared with numerical and experimental data available in the literature.

Keywords: Second-order effects; Partial shear connection; Concentrated plasticity; Steel-concrete composite frames; Interaction curves

1 Introduction

Several sources of non-linearities are decisive in obtaining the bearing capacity of steel-concrete composite structural elements. Despite the widespread use of composite systems, precise numerical procedures for their analysis and design have not evolved in the same way as for steel structures. Thus, the study of numerical formulations that are increasingly efficient is a continuous and necessary process. Although some formulations are already stable for the simulation of geometric and material nonlinearity in this type of structure, cracking and partial interaction are still sources of study in formulations concentrated at nodal points.

To simulate the effect of partial shear connection, Dall'Asta and Zona [1] reported the use of displacement-based formulations presents problems related to locking phenomena. These phenomena are linked to an unrealistic stiffening of the structure, for example, the loss of precision in assessing the effect of slip on the connection (slip locking). Battini et al. [2] chose to use the stiffness matrix based on the exact solution of the equations that govern the problem of composite beams with partial shear connection. Sousa Jr et al. [3] concentrated their solutions on the degree of the used displacement interpolation functions.

In the basic conception of the refined plastic hinge method (RPHM), cracking cannot be considered since the method was developed for homogeneous isotropic materials. Thus, an explicit equation for the crack simulation is necessary.

Still little explored in the analysis of composite elements with partial longitudinal interaction, concentrated plasticity was found in only three studies [4–6]. In all these works, the numerical simulation of the partial shear connection is introduced in the models in the same way. The simulation is done using the considerations of the American standard [7]. However, the description of the composite beam elements and the geometric non-linear formulation are completely different from the present work.

The present study aims to implement a displacement-based numerical formulation for the non-linear simu-

lation of composite and bare steel structural elements. The non-linear effects are concentrated at the nodal points using RPHM. The effects of cracking and partial interaction will be explicitly considered at the moment of inertia of the section [8, 9]. Direct consideration of the degree of composite action eliminates localized non-linear processes avoiding the locking phenomenon.

2 Finite element formulation

In the present work, the displacement-based formulation with concentrated plasticity in the nodal points is applied. In this case, the axial and flexural stiffness degradation occurs exclusively at the FE nodes. Then, the method is presented, introducing the material nonlinearity only. Some considerations and simplifications of this formulation can be seen in [10, 11].

In the structural system modelling, the hybrid beam-column finite element of length L , delimited by nodal points i and j (Figure 1), is used. This element has zero-length pseudo rotational springs at its ends, which are responsible for the plasticity simulation by means of the parameter S_p , discussed in Section 3. The finite element is referenced to the co-rotational system where the degrees of freedom are the rotations at nodes i and j , given by θ_i and θ_j , and the axial displacement in j , δ . The terms M_i , M_j and P represent the bending moments and the axial force in the respective degrees of freedom.

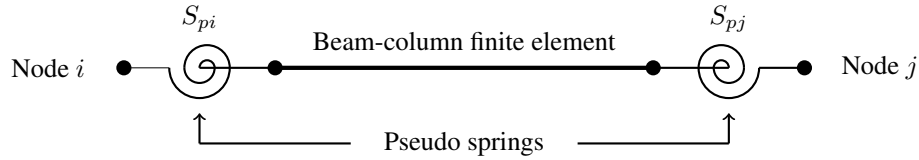


Figure 1. Finite element with pseudo-springs

$$\begin{Bmatrix} \Delta N \\ \Delta M_{pi} \\ \Delta M_{pj} \end{Bmatrix} = \begin{bmatrix} k_{11} & 0 & 0 \\ 0 & S_{pi} - \frac{S_{pi}^2 (S_{pj} + k_{33})}{\beta} & \frac{S_{pi} k_{23} S_{pj}}{\beta} \\ 0 & \frac{S_{pj} k_{32} S_{pi}}{\beta} & S_{pj} - \frac{S_{pj}^2 (S_{pi} + k_{22})}{\beta} \end{bmatrix} \begin{Bmatrix} \Delta \delta \\ \Delta \theta_{pi} \\ \Delta \theta_{pj} \end{Bmatrix} \quad (1)$$

in which $\beta = (S_{pi} + k_{22})(S_{pj} + k_{33}) - k_{32}k_{23}$.

The terms k_{11} , k_{22} , k_{23} , k_{32} , and k_{33} are components of the beam-column stiffness matrix element, without the pseudo-springs, described as [10]:

$$\begin{aligned} k_{11} &= \frac{E_s A}{L} & k_{22} &= \frac{E_s (3I_{eff,i} + I_{eff,j})}{L} \\ k_{23} &= k_{32} = \frac{E_s (I_{eff,i} + I_{eff,j})}{L} & k_{33} &= \frac{E_s (I_{eff,i} + 3I_{eff,j})}{L} \end{aligned} \quad (2)$$

where E_s is the steel modulus of elasticity, A is the homogenized area of the section, I_{eff} is the modulus of inertia as discussed on Section 4, measured in nodes i and j , and L is the finite element length.

3 Pseudo springs flexural stiffness

The limits of uncracked, elastic or plastic states are defined by the by the moment-curvature relationship [10]. In this nonlinear procedure, the initial cracking moment M_{cr} , the initial yield moment M_{er} and the full yield moment M_{pr} can be easily obtained.

Figure 2 illustrates three interaction curves for a specific cross-section: the full yield curve – indicates the bearing capacity; the initial yield curve – defines the elastic region; and the initial cracking curve – delimits the uncracked state of the cross-section. These curves are the result of a combination of axial force and a bending moment acting around one of the main axes bending. For bare steel or steel-concrete composite columns, the procedure to obtain these three curves is described in Lemes et al. [11]. For composite beam, Lemes [10] presented the methodology to determine the cracking, elastic and plastic bending moments in this element.

In Figure 2, it is also possible to observe four regions. Thus, expression definitions for the simulation of pseudo-spring stiffness in each of the described regions are required.

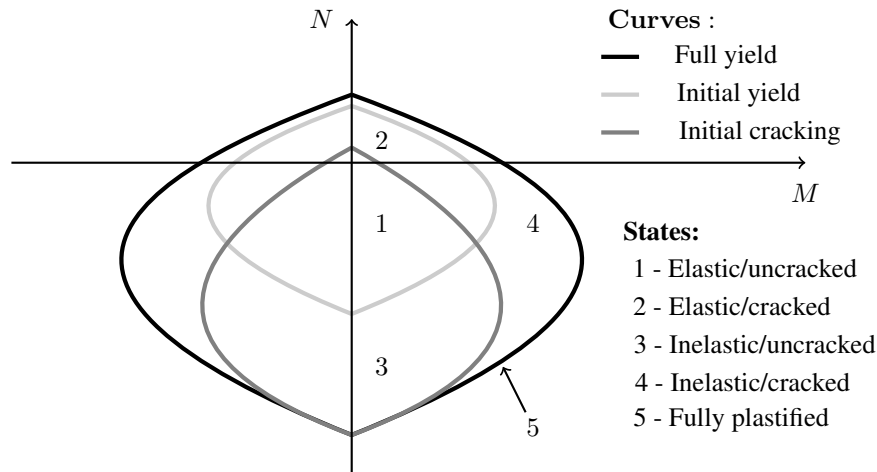


Figure 2. Interaction curves for cross section flexural stiffness degradation

According to the classical RPHM, three equations define the pseudo-spring stiffness for the previously mentioned regions. In regions 1 and 2, it is observed that the section is in an elastic regime. In regions 3 and 4, there can be noticed that the section is in a stiffness degradation process due to plastic strains. And finally, for when the fully plastified section occurs (region 5). For a given axial force-bending moment combination, S_p is defined as follow:

$$\begin{aligned}
 &\text{if } M \leq M_{er} : S_p = 1 \times 10^{10} \\
 &\text{if } M_{er} \leq M \leq M_{pr} : S_p = \frac{E_s I_{eff}}{L} \left(\frac{M_{pr} - M}{M - M_{er}} \right) \\
 &\text{if } M_{pr} \leq M : S_p = 1 \times 10^{-10}
 \end{aligned} \tag{3}$$

in which L is the finite element length and $E_s I_{eff}$ is the section's flexural stiffness, considering the cracking, as discussed below.

Note that, by the value described in Eq. 3, there is no possibility of simulating cracking and partial shear connection in the elastic regime. This adjustment is made in the following section.

4 Moment of inertia

Branson and Metz [8] proposed a simple equation for the effective moment of inertia evaluation of RC sections in a cracking state. This equation is used by some design codes, such as NBR 6118 [12]. The effective moment of inertia, $I_{eff,c}$, is given by:

$$\begin{aligned}
 &\text{if } M \leq M_{cr} : I_{eff,c} = I_c \\
 &\text{if } M > M_{cr} : I_{eff,c} = \left(\frac{M_{cr}}{M} \right)^3 I_c + \left[1 - \left(\frac{M_{cr}}{M} \right)^3 \right] I_{cr} \quad I_{eff} \leq I_c
 \end{aligned} \tag{4}$$

where M_{cr} and M are, respectively, the initial cracking bending moment and the bending moment acting on the section, I_c is the intact section moment of inertia, and I_{cr} is the cracked moment of inertia of the section evaluated in the critical point of moment-curvature relationship [10].

Considering the partially conjunct action with concrete slab and steel section, the effective moment of inertia, I_{eff} , can be determined as a directly function of degree of interaction, η_i . Thus [9]:

$$I_{eff} = I_{steel} + \sqrt{\eta_i} (I_{tr} - I_{steel}) \tag{5}$$

in which I_{steel} and I_{tr} are moment of inertia of steel and homogenized cross sections, respectively. The homogenized moment of inertia is calculated by the direct relation of $I_{eff,c}$ and I_{steel} .

5 Calibration of the numerical formulation

The calibration of the presented numerical formulation is made by three analysis of steel-concrete composite structures. Thus, a continuous composite beam with partial shear connection is simulated comparing the experimental and numerical data presented in literature. After, two analysis are made in composite portal frame. The first analysis considers steel columns and a composite beam with full interaction. Finally, the last analysis addresses the same frame but with concrete encased steel columns.

5.1 Continuous composite beam with partial shear connection

The first application for model calibration is made considering a continuous steel-concrete composite beam with partial interaction. In this simulation, the concrete was considered to have a compressive strength of 2.46 kN/cm^2 and the yield strength of the steel was taken as 29.11 kN/cm^2 , disregarding the strain hardening. The areas of the bars present in the concrete slab A_{b1} and A_{b2} are equal to 8 cm^2 and 3.16 cm^2 in the region of hogging moment and equal to 0 cm^2 and 1.6 cm^2 in the sagging moment region. Figure 3 illustrates the equilibrium paths of the continuous composite beam. Considering the other data provided in this same figure, it is possible to verify a satisfactory approximation of the numerical and experimental [13] results.

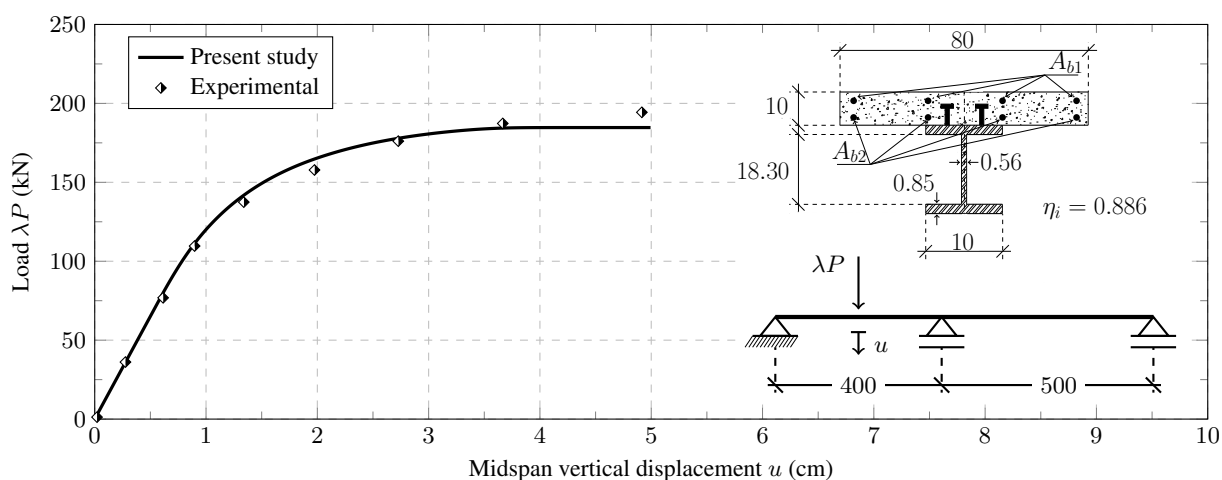


Figure 3. Equilibrium paths for continuous composite beam (dimensions in cm)

5.2 Composite portal frame

Now, a simple frame illustrated in Fig. 4 is analyzed and compared with literature numerical results [5]. The structure has 5 meters of both height and span. The columns are constituted by $W12 \times 50$ steel section and the beam with $W12 \times 27$. The concrete slab has a height of 102 mm and a width of 1219 mm. The columns are initially considered as bare steel and encased steel column in a second analysis, presenting a composite square section with a base equal to 400 mm.

Two analyzes will be carried out: structure with steel columns and composite beam (SC) and the totally composite structural system (CC). The equilibrium paths for these systems are defined by varying the incremental load in relation to the displacement u at the top of the right column. For steel, a yield strength f_y equal to 24.82 kN/cm^2 and a Young's modulus taken as 20000 kN/cm^2 are considered. The compressive strength of concrete, f_c , adopted is 1.6 kN/cm^2 .

Figure 5 shows the load-displacement curves for the described two cases. Observing Fig. 5(a), it can be concluded that the methodology used in this work is consistent with the results obtained by Iu et al. [5]. It is possible to verify in Fig. 5(b) that the stiffness sharp drop obtained in Lemes et al. [14], highlighted in this figure, is corrected with the introduction of the stiffness degradation of the section due to cracking, by the Branson Equation.

It can be concluded the proposed formulation satisfactorily captures the behavior of steel-concrete composite beams with full and partial interaction, as well as the behavior of composite and bare steel columns.

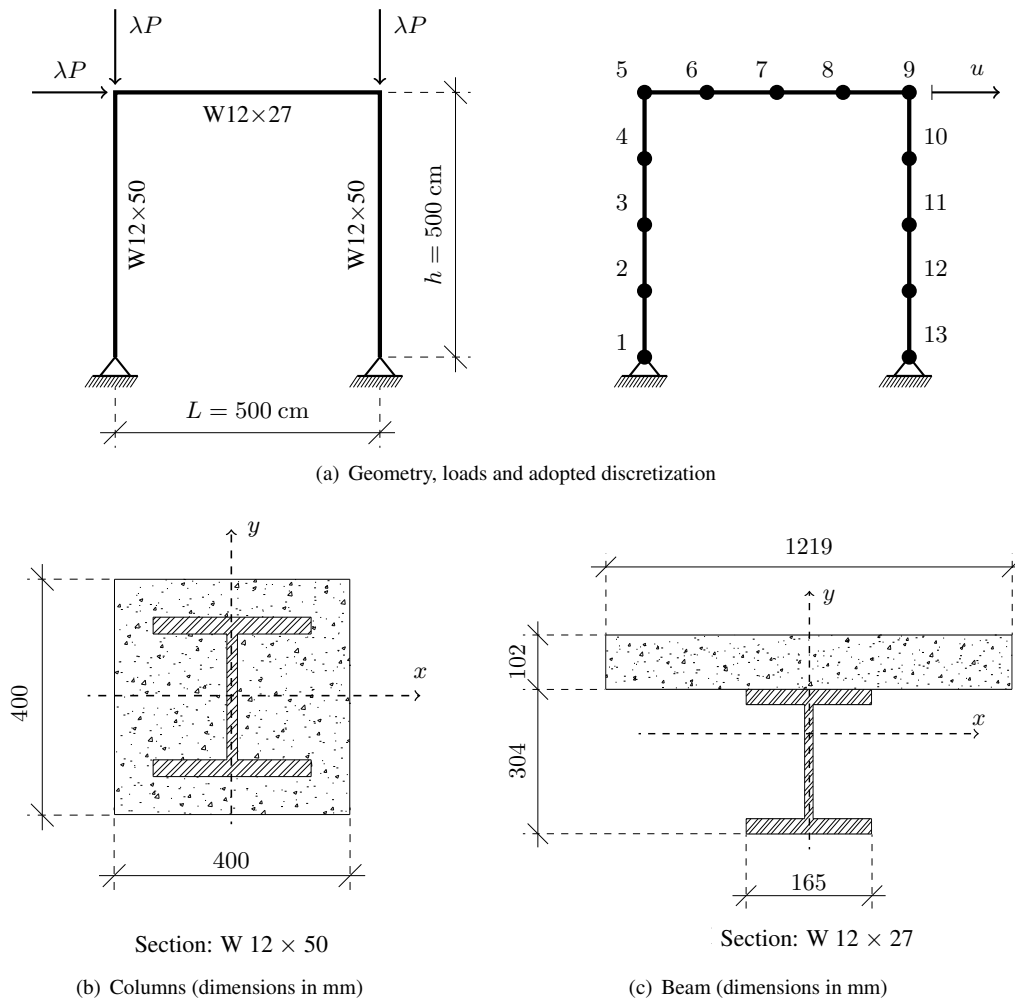


Figure 4. Composite portal frame

6 Numerical application

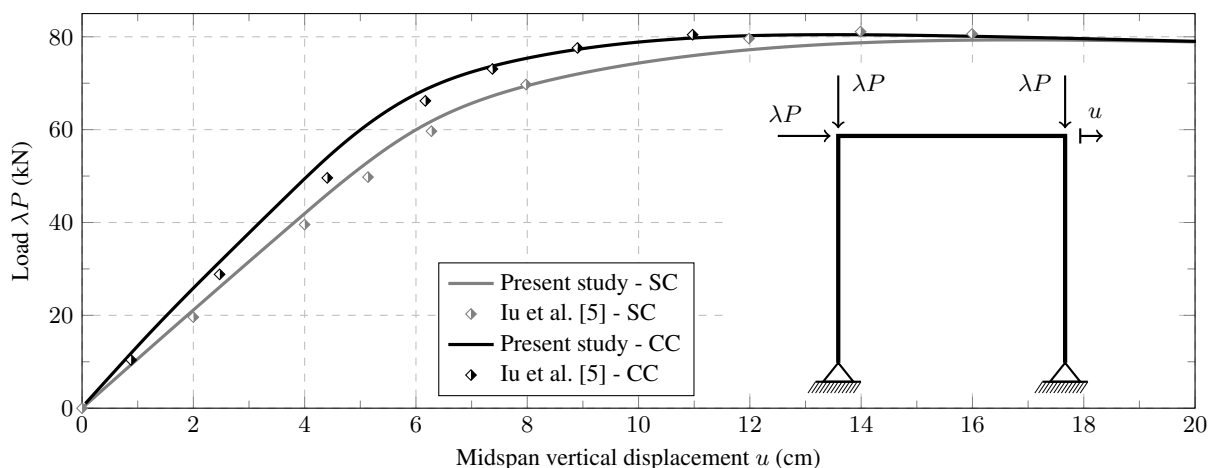
After verifying the accuracy of the numerical formulation presented in the present work, a study of the behavior of the composite portal frame with steel columns and steel-concrete composite beam is made. This frame is exactly the same one tested in the item 5.2 considering the bare steel columns. In this analysis, various degrees of interaction are applied to the beam, and the equilibrium paths is obtained for each case, as presented in Fig. 6. The minimum value ($\eta_i = 0.4$) was defined based on NBR 8800 [9].

Considering the presented formulation, the partial shear connection has little influence on the initial stiffness of the system, as highlighted in Fig. 6. It is also possible to verify that the onset of stiffness degradation for all frames occurs at different times, Fig. 6. In all cases, the most requested node is node 9 (right end of the beam), thus, it presents stiffness degradation before the others. And at the load limit point, this node is plastified in all the frames.

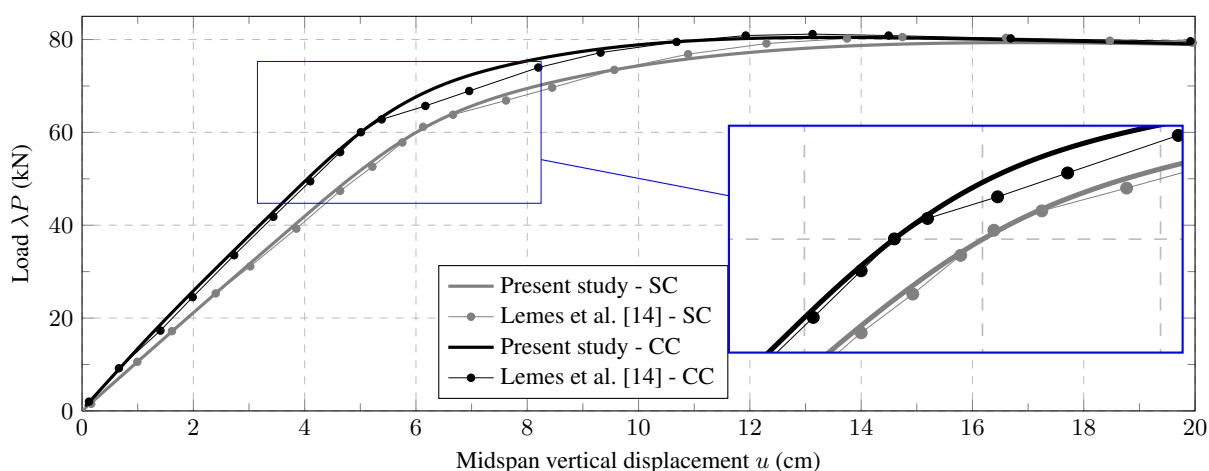
Due to the drop in the bearing capacity of the beam - since the greatest degradation occurs in the beam - as the lower the degree of composite action as the lower the system's resistant capacity.

7 Conclusions

A methodology of nonlinear analysis of steel-concrete composite frames was presented in the present work. From the sources of non-linearity, in the present work, geometric, material and shear connection between the steel section and the concrete slab were considered. In this sense, these effects were concentrated at the nodal points using the refined plastic hinge method (RPHM). The classic RPHM was changed by separating the degradation of stiffness in two approaches: plastification was evaluated by means of pseudo-springs placed at the finite elements ends; and concrete cracking and partial shear connection were considered based on the Branson and Metz [8] and



(a) Comparison with Iu et al. [5] results



(b) Comparison with Lemes et al. [14] results

Figure 5. Equilibrium paths for composite portal frame

NBR 8800 [9] equations, respectively.

Two examples of calibration of the numerical formulation were presented. The first approached a continuous composite beam with partial interaction. The results found in this article were consistent with the experimental data obtained by Ansourian [13]. It was possible to observe good convergence in the three phases of the load-displacement curve: elastic, elasto-plastic and plastic regimes. Additionally, there were no problems related to the locking phenomena. Thus, consequently, the limit load obtained in the numerical model was visually close to the experimental value. In a second step, a simple frame was analyzed. This frame had two configurations: bare steel columns and composite beam; concrete encased steel columns and composite beam. In both cases the beam presents full interaction and the results converged to the data obtained by Iu et al. [5]. It should be noted that the formulation presented here corrected the sharp drop in stiffness observed in the work of Lemes et al. [14].

A simple study was carried out in sequence where the frame that had already been calibrated was modified considering the composite beam with partial interaction. Various degrees of composite action were tested to analyze the formulation behavior. The results were consistent with the expected, highlighting the validity of the formulation.

Finally, it is concluded that the information presents satisfactory results for elements required and small frames. It should be tested in the future on larger structures including the effect of semi-rigid connections.

Acknowledgements

The authors would like to thank CAPES and CNPq (Federal Research Agencies), Fapemig (Minas Gerais State Research Agency), UFLA and UFOP for their support during the development of this work.

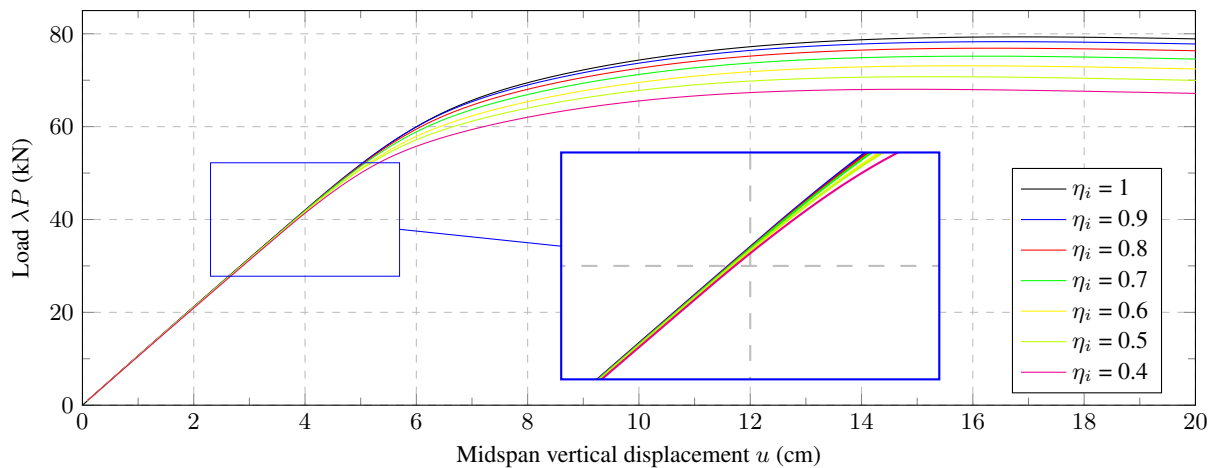


Figure 6. Equilibrium paths for portal composite frame with various degree of composite action

Authorship statement

The authors hereby confirm that they are the sole liable persons responsible for the authorship of this work, and that all material that has been herein included as part of the present paper is either the property (and authorship) of the authors, or has the permission of the owners to be included here.

References

- [1] Dall'Asta, A. & Zona, A., 2004a. Slip locking in finite elements for composite beams with deformable shear connection. *Finite Elements in Analysis and Design*, vol. 40, pp. 1907–1930.
- [2] Battini, J. M., Nguyen, Q. H., & Hjiij, M., 2009. Non-linear finite element analysis of composite beams with interlayer slip. *Computers and Structures*, vol. 87, pp. 904–912.
- [3] Sousa Jr, J. B. M., Oliveira, C. E. M., & Silva, A. R., 2010. Displacement-based nonlinear finite element analysis of composite beam-columns with partial interaction. *Journal of Constructional Steel Research*, vol. 66, pp. 772–779.
- [4] Liew, J., Chen, H., & Shanmugam, N., 2001. Inelastic analysis of steel frames with composite beams. *Journal of Structural Engineering*, vol. 127, n. 2, pp. 194–202.
- [5] Iu, C., Bradford, M., & Chen, W., 2009. Second-order inelastic analysis of composite framed structures based on the refined plastic hinge method. *Engineering Structures*, vol. 31, pp. 799–813.
- [6] Iu, C. K., 2016. Nonlinear analysis for the pre and post yield behaviour of a composite structure with the refined plastic hinge method. *Journal of Constructional Steel Research*, vol. 119, pp. 1–16.
- [7] AISC LRFD, 2016. Specification for structural steel buildings. *American Institute of Steel Construction, Chicago, IL*.
- [8] Branson, D. & Metz, G., 1963. Instantaneous and time-dependent deflections of simple and continuous reinforced concrete beams. Technical report, Auburn: Dept. of Civil Engineering Auburn Research Foundation, Auburn University, Auburn: Dept. of Civil Engineering and Auburn Research Foundation, Auburn University.
- [9] NBR 8800, 2008. Projeto de estruturas de aço e de estruturas mistas de aço e concreto de edifícios. *Associação Brasileira de Normas Técnicas*.
- [10] Lemes, Í. J. M., 2018. *Advanced numerical study of steel, concrete and steel-concrete composite structures*. PhD thesis, Federal University of Ouro Preto, Ouro Preto, Brazil.
- [11] Lemes, Í. J. M., Barros, R. C., Silveira, R. A. M., Silva, A. R. D., & Rocha, P. A. S., 2018. Numerical analysis of rc plane structures: a concentrated nonlinear effect approach. *Latin American Journal of Solids and Structures*, vol. 15, n. 2.
- [12] NBR 6118, 2014. Projeto de estruturas de concreto - procedimento. *Associação Brasileira de Normas Técnicas*.
- [13] Ansourian, P., 1981. Experiments on continuous composite beams. *Proceedings of the Institution of Civil Engineer*, vol. 71, n. 2, pp. 25–51.
- [14] Lemes, Í. J. M., Silva, A. R. D., Silveira, R. A. M., & Rocha, P. A. S., 2017b. Numerical analysis of nonlinear behavior of steel concrete composite structures. *Ibracon Structures and Materials Journal*, vol. 10, n. 1, pp. 53–83.